

## Article

# A Comparative Approach Study on the Thermal and Calorimetric Analysis of Fire-Extinguishing Powders

An-Chi Huang \* , Fang-Chao Cao and Xin-Yue Ma

School of Safety Science and Engineering, Changzhou University, No. 21, Gehu mid-Rd., Wujin Dist., Changzhou 213164, China; 15216402008@163.com (F.-C.C.); b23200837004@smail.cczu.edu.cn (X.-Y.M.)

\* Correspondence: huangac@cczu.edu.cn

**Abstract:** This study offers a comprehensive evaluation of the effectiveness of expansible graphite (EG) and potassium bicarbonate ( $\text{KHCO}_3$ ) in suppressing metal fires, which are known for their high intensity and resistance. Our assessment, utilizing thermogravimetric analysis (TGA), Fourier transform infrared spectroscopy (FTIR), X-ray diffraction (XRD), and scanning electron microscopy (SEM), revealed that compositions of EG– $\text{KHCO}_3$  can endure temperatures of up to 350 °C, indicating their thermal resilience. The 3:1 EG– $\text{KHCO}_3$  mixture demonstrated exceptional performance in fire suppression tests by extinguishing sodium flames in a mere 20 s, using approximately 50 g of the agent. This highlights a substantial improvement in efficiency. In addition, FTIR analysis identified important gaseous compounds released during decomposition, while XRD and SEM techniques confirmed the advantageous insertion of  $\text{KHCO}_3$  into the EG matrix, enhancing its resistance to heat and chemical reactions. The mixture with a ratio of 3:1 also demonstrated a higher cooling rate of 2.34 °C/s within the temperature range of 350 to 200 °C. The results emphasize the potential of EG– $\text{KHCO}_3$  compositions, specifically in a 3:1 ratio, for efficient fire management by integrating fire suppression, heat resistance, and quick cooling. Subsequent investigations will prioritize the evaluation of these compositions across different circumstances and the assessment of their environmental and industrial viability.

**Keywords:** expansible graphite (EG); potassium bicarbonate ( $\text{KHCO}_3$ ); sodium flames; gaseous compounds; cooling rate



**Citation:** Huang, A.-C.; Cao, F.-C.; Ma, X.-Y. A Comparative Approach Study on the Thermal and Calorimetric Analysis of Fire-Extinguishing Powders. *Safety* **2024**, *10*, 31. <https://doi.org/10.3390/safety10010031>

Academic Editor: Raphael Grzebieta

Received: 4 November 2023

Revised: 18 January 2024

Accepted: 12 March 2024

Published: 15 March 2024



**Copyright:** © 2024 by the authors. Licensee MDPI, Basel, Switzerland. This article is an open access article distributed under the terms and conditions of the Creative Commons Attribution (CC BY) license (<https://creativecommons.org/licenses/by/4.0/>).

## 1. Introduction

Fire-extinguishing powders play a crucial role in the domain of fire safety, providing a varied approach to managing and suppressing different categories of fires, particularly those associated with combustible metals and electrical apparatus [1]. These powders function by establishing a physical barrier that separates the fire from oxygen, thereby interrupting the process of combustion [2]. The efficacy of these powders relies on various parameters, such as their chemical composition, particle size, and the technique of administration, thus requiring a comprehensive examination of their properties and behaviors [3].

Numerous research studies have extensively investigated the thermal properties of fire-extinguishing powders, providing insights into various elements, such as melting points, heat capacities, and thermal disintegration [4]. Furthermore, the utilization of calorimetric investigations has contributed valuable insights into the thermodynamic properties of these powders, specifically in relation to their heat of reaction and heat of creation [5,6]. These studies have enhanced our understanding of the energy dynamics involved in the process of fire suppression. Nevertheless, the current body of research lacks a thorough examination of the thermal and calorimetric characteristics of powders, namely those based on expansible graphite (EG) and potassium bicarbonate ( $\text{KHCO}_3$ ) [7,8].

The crucial significance of fire-extinguishing powders in ensuring fire safety highlights the essential requirement for a comprehensive understanding of their thermal and calorimetric characteristics. This is particularly relevant for powders that are manufactured with

EG and  $\text{KHCO}_3$ , as these powders are commonly used, but there is a limited comprehensive understanding of their fire suppression mechanisms and effectiveness. The lack of such expertise presents a notable obstacle to maximizing their utilization in fire suppression and safety.

The objective of this study is to enhance the scientific understanding of fire suppression by examining the interaction between the thermodynamic and calorimetric properties of fire-retardant materials, specifically in difficult situations, such as metal fires. This research aims to enhance theoretical understanding and explore new possibilities for developing fire suppression methods that are more efficient and environmentally friendly by focusing on the distinct characteristics of EG and  $\text{KHCO}_3$ . We aim to fill the current knowledge deficit by conducting a comprehensive analysis of the thermal and calorimetric characteristics of fire-extinguishing powders containing EG and  $\text{KHCO}_3$ . This endeavor seeks to greatly enhance the composition and techniques of fire suppression, thereby improving the effectiveness of fire prevention methods. The findings of this study are expected to provide valuable insights for both the academic discourse and practical implementation of fire-extinguishing powders, with the goal of enhancing the effectiveness and dependability of fire suppression solutions.

In order to accomplish these goals, our research conducts a thorough analysis of various fire-suppressing powders, specifically emphasizing formulations that include EG and  $\text{KHCO}_3$ . We will evaluate the thermal properties and qualities of these powders using a sophisticated X-ray diffraction (XRD) analytical method [9]. This approach will facilitate a comprehensive analysis of the crystalline structures of the powders and their ability to withstand variations in temperature. In addition, the study will conduct a thorough calorimetric analysis using thermogravimetric (TG) and differential thermal analysis (DTA) techniques to examine the thermal transitions and reactions of the samples [10]. In addition, we will utilize an integrative approach that combines TG research with Fourier transform infrared spectroscopy (FTIR) to gain a more comprehensive understanding of the mechanisms through which these powders extinguish fires [11]. By employing these techniques in combination, a thorough comprehension of the interplay between these particles and fire, as well as heat, will be achieved.

## 2. Materials and Experiments

### 2.1. Materials

The EG utilized in this study was procured from a reliable supplier, renowned for providing graphite goods of exceptional quality. The EG that was chosen exhibited a purity level of 99.5% and had a median particle size of 50  $\mu\text{m}$ , as stated in the powder literature [12]. In order to uphold its quality and mitigate the risk of contamination, the EG was stored within a controlled environment, characterized by low humidity and cool temperatures. All reagents and chemicals employed in this study were of analytical quality, ensuring the highest level of purity and dependability. These substances were used as received, without undergoing any additional purification processes. The used instruments, such as calorimeters, spectrometers, and microscopes, were subjected to regular maintenance and calibration procedures in order to uphold the precision and dependability of the obtained outcomes. A set of five distinct concentration ratios of EG– $\text{KHCO}_3$  were created for the purpose of analysis. These ratios are 0:1, 1:0, 1:1, 3:1, and 9:1, as listed in Table 1.

**Table 1.** Compositions of three EG– $\text{KHCO}_3$  powders.

Material Designation	EG	$\text{KHCO}_3$
Percentage (%)	50%	50%
	75%	25%
	90%	10%

During the process of sample preparation, the EG was precisely measured by means of a high-precision balance. The samples were subsequently subjected to a series of treat-

ments, including controlled heating, cooling, and chemical changes, in accordance with established protocols. The study utilized a comprehensive and methodical experimental design to investigate the intricate characteristics of EG. The research maintained the study's strength and credibility by establishing precise definitions for independent, dependent, and controlled variables. The data collection process was executed with utmost precision, employing advanced statistical techniques to conduct a thorough analysis that aimed to find noteworthy trends, patterns, and anomalies.

## 2.2. Experiments

TG was employed to thoroughly investigate the thermal properties of the five different ratios of synthesized compositions of EG and  $\text{KHCO}_3$ . The heating rate of TG was set at  $10\text{ }^\circ\text{C}/\text{min}$ , and the heating range was from 30 to  $900\text{ }^\circ\text{C}$  [13]. TG analysis used nitrogen to create an inert atmosphere. The non-reactivity of nitrogen prevents oxidation and combustion in ambient air. We can observe the decomposition and interaction of EG– $\text{KHCO}_3$  mixtures under real-world fire suppression conditions without external oxidative influences, which is necessary to accurately assess their thermal behavior and stability. The utilization of this sophisticated analytical methodology facilitated the accurate quantification of the mass reduction of the specimens in relation to varying temperatures. By means of this investigation, the research team successfully ascertained the temperatures at which decomposition commenced, the temperature interval during which significant weight loss transpired, and the ultimate percentage of residual weight. The TG curves exhibited discernible phases of heat degradation, with each phase corresponding to certain chemical processes occurring inside the EG– $\text{KHCO}_3$  composite. The temperatures at which these stages were seen were meticulously recorded, facilitating a comprehensive understanding of the thermal stability and breakdown properties of the materials.

The fire-suppression characteristics of the EG– $\text{KHCO}_3$  compositions were thoroughly examined in a controlled experimental setting. The experimental configuration was carefully devised to emulate fire scenarios encountered in real-world settings, hence ensuring the dependability and applicability of the findings. A controlled ignition source was employed to create a fire, thereby replicating a conventional combustion process. Various concentrations of EG– $\text{KHCO}_3$  compositions were delivered to the fire source upon ignition. In this context, 'concentration' refers to the specific ratio of each component (EG and  $\text{KHCO}_3$ ) relative to the overall volume or mass of the extinguishing agent, emphasizing the exact amount of each substance utilized in our experiments. The researchers conducted a thorough examination and documentation of the duration required for each composition to successfully extinguish the fire, the quantity of composition necessary for efficient suppression, and the characteristics and quantity of residues remaining after extinguishment. The aforementioned observations played a pivotal role in ascertaining the most favorable concentration of EG– $\text{KHCO}_3$  for efficient fire suppression and comprehending its mechanism of action.

Each formulation underwent five distinct trials to ensure uniformity in fire intensity and environmental conditions. During each trial, we utilized 50 g of sodium and recorded the duration required for complete cessation of combustion. The experiments were carried out under uniform conditions, with a regulated temperature and humidity level, and a consistent quantity of extinguishing agent was utilized for each trial. The consistent decrease in the time required to extinguish and the amount of extinguishing agent used in each trial highlights the efficacy of the 3:1 EG– $\text{KHCO}_3$  composition.

In order to further investigate the molecular-level fire-suppression mechanism of EG– $\text{KHCO}_3$ , the research team conducted an analysis of the gaseous byproducts that are generated during its decomposition. The analytical approach selected for this purpose was FTIR, due to its capability to discern certain chemical bonds and functional groups. Through the examination of the FTIR spectra, the research team successfully determined the main gases that are emitted during the process of decomposition at the temperature of 135, 210, and  $580\text{ }^\circ\text{C}$  [14,15]. These temperatures were strategically selected, based on

their significance in the thermal degradation process of the EG–KHCO<sub>3</sub> mixtures. The first temperature corresponds to the initial decomposition stage, where the preliminary breakdown of compounds occurs. The second temperature represents a midpoint in the thermal degradation process, where major chemical transformations are hypothesized. The final temperature is chosen to observe the end-stage byproducts, providing insights into the complete degradation profile. Additionally, they were able to ascertain the relative amounts of these gases and investigate their possible contributions to the fire-suppression mechanism. The comprehension of EG–KHCO<sub>3</sub> at the molecular level has yielded significant insights on its effectiveness and safety as a fire-suppression agent.

The study utilized high-resolution cameras to visually record the fire-suppression process, as depicted in Figure 1, thereby enhancing the quantitative data collected. The presented visual documentation presents a chronological representation of the interactions between the compositions of EG–KHCO<sub>3</sub> and the fire source. This documentation aims to provide a thorough comprehension of the suppression operation, encompassing the agent's initial contact with the fire, until its ultimate extinguishment. The inclusion of visual evidence in the analysis served to reinforce the quantitative findings, thereby enhancing the comprehensive understanding of the operational mechanisms involved in fire suppression [16].

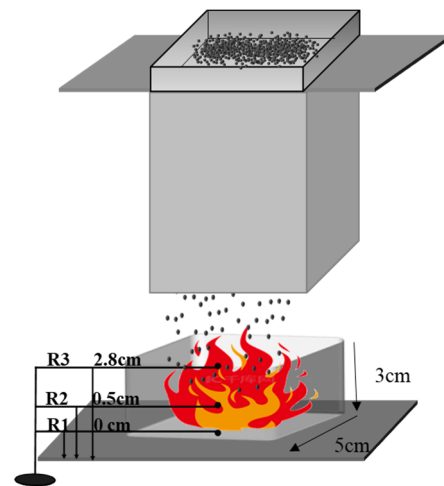


**Figure 1.** Fire-suppression process instrument.

The schematic diagram in Figure 1 illustrates the experimental setup for the fire suppression study, conducted in a confined room with dimensions of 1.2 m (width), 0.55 m (length), and 1.9 m (height). The establishment of a controlled environment was of utmost importance in order to uphold consistent settings, hence facilitating a precise assessment of the fire-suppression procedure. The presence of a highly effective ventilation system was vital during the course of the experiment in order to effectively remove the corrosive smoke generated during the process of burning, thereby guaranteeing the well-being and security of all those participating in the experiment.

At the core of the experimental configuration resided a combustion chamber composed of stainless steel, with dimensions of 5 cm × 5 cm × 3 cm. The experimental setup involved the introduction of metallic sodium into a designated chamber, which was subsequently subjected to heat using a heating plate. This process induced a phase transition from a solid to a molten state, resulting in the formation of a sodium pool fire. This particular situation is representative of a class D fire, which is well-known for its high intensity and the difficulties associated with extinguishing it. The temperature fluctuations observed during the combustion of sodium were carefully monitored by employing three thermocouples, strategically positioned above the sodium pool. This enabled the acquisition of real-time thermal output data, which played a crucial role in evaluating the efficacy of the fire control techniques being investigated [17,18].

A vibrating sieve mechanism was mounted above the combustion chamber. The inclusion of this particular component played a crucial role in facilitating the uniform and uninterrupted dispersion of the fire-suppressing powder across the area affected by the fire. The vibration frequency of the sieve was meticulously regulated to ensure uniform dispersion, while its placement, at a distance of approximately 15 cm above the pan, was intended to maximize coverage and enhance the efficacy of fire suppression.

### 2.3. Quality Control and Validation

In order to assure the highest level of precision and dependability in the obtained outcomes, all equipment included in the study underwent meticulous calibration processes before each experimental trial, and their calibration statuses were consistently validated. In order to establish the dependability and replicability of the findings, a series of replications were conducted for each experiment. The acquired data underwent thorough scrutiny to ensure precision and coherence before undergoing subsequent analysis. A comprehensive examination of the available literature was conducted to compare the findings of this study with previous research, enabling a detailed analysis of the similarities, differences, and unique contributions of this study to the current knowledge in the field [19,20].

## 3. Results and Discussion

This part provides a comprehensive examination of the conducted tests, with a specific emphasis on the thermal characteristics of EG–KHCO<sub>3</sub> compositions, their effectiveness in suppressing fires, the gaseous byproducts generated during their decomposition, and the visual depiction of the fire extinguishment process.

### 3.1. Thermal Decomposition Analysis

TG was employed to investigate the thermal stability and breakdown properties of EG–KHCO<sub>3</sub>. The thermal decomposition stages of the materials under a nitrogen atmosphere are indicated by the TG-DTG curves, as depicted in Figure 2. The findings demonstrate clear phases of mass reduction, emphasizing the compositions' thermal resilience and sites of disintegration. Thermal resilience refers to the capacity of EG–KHCO<sub>3</sub> compositions to retain their structural integrity and effectiveness in suppressing fires when exposed to elevated temperatures. This encompasses their ability to withstand thermal degradation, prevent substantial chemical modifications, and maintain optimal performance in fire situations. Table 2 presents a comprehensive examination of the residual mass and peak rate observed during the primary mass loss of EG and modified EG powders. This research provides insights into the various stages of decomposition and their associated temperatures. EG displayed a transition at the temperature of 212.42 °C and another one at 614.95 °C, whereas the mixture with a ratio of 3:1 exhibited transitions at the temperatures of 35.42 °C, 228.19 °C, and 615.71 °C. The residual percentages and rates of change at the highest points in this range offer valuable insights into the thermal stability and reaction kinetics of the materials. In order to effectively assess the effectiveness of fire suppression, we specifically targeted this temperature range to capture the most important thermal changes. This was demonstrated by the residue percentages of 65.34% for EG and 68.49% for the 3:1 mixture in the later stages. The TG analysis presented in the figures commences by examining the compositions of EG–KHCO<sub>3</sub>. These compositions exhibit a consistent weight until reaching a certain temperature threshold, indicating an initial state of thermal stability. With an increase in temperature, there is a noticeable decrease in weight, which is indicated by a peak in the differential thermal gravity curve. This peak represents an important stage in the decomposition of expansible graphite. The decomposition phase is noticeably altered when potassium bicarbonate is present, indicating an interaction that improves the composite material's ability to withstand high temperatures. The residual weight percentage observed at high temperatures indicates the presence of a stable residue, which is likely responsible for the material's effectiveness in suppressing fires. When analyzing the thermal properties of the mixtures in comparison to pure EG, the inclusion

of  $\text{KHCO}_3$  seems to create a synergistic impact that alters the thermal degradation pattern, suggesting enhanced fire retardant abilities. This observation is significant because it corresponds with the desired result of increased effectiveness in suppressing metal fires, which is particularly important in situations where the ability of the suppression agent to withstand high temperatures is of utmost importance. The comprehensive analysis of TG-DTG concludes by identifying the 3:1 EG– $\text{KHCO}_3$  ratio as a highly promising composition. This composition offers improved thermal stability and has the potential to enhance fire suppression performance.

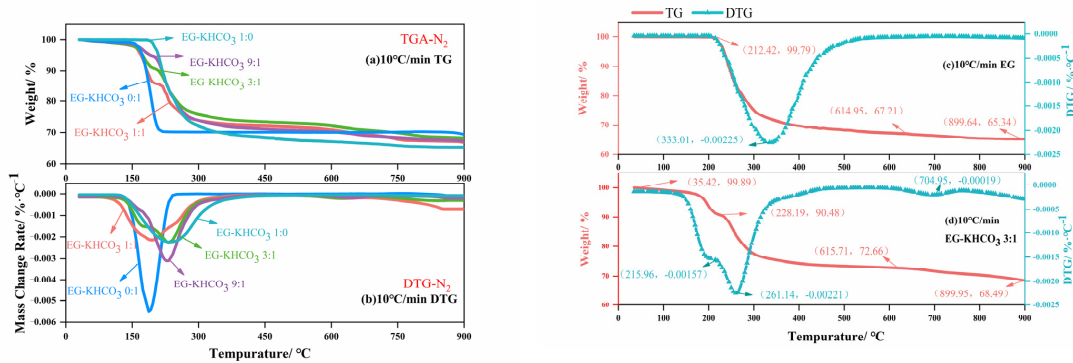


**Figure 2.** TG-DTG curves of five samples placed in a nitrogen atmosphere at a heating rate of 10 °C/min; (a) TG of all samples, (b) DTG of all samples, (c) TG-DTG of EG, and (d) TG–DSC of EG– $\text{KHCO}_3$ .

**Table 2.** Stages of residual mass and peak rate during main mass loss of EG and modified EG powders.

Samples	Arguments	First Stage	Second Stage	Third Stage
EG	$T_0$ (°C)	212.42	614.95	–
	Residue (%)	67.21	65.34	–
	Peak rate (%/°C)	0.0022	–	–
EG– $\text{KHCO}_3$ 3:1	$T_0$ (°C)	35.42	228.19	615.71
	Residue (%)	90.48	72.66	68.49
	Peak rate (%/°C)	0.0016	0.0022	0.0002

### 3.2. Fire Extinguishing Efficacy

The efficacy of EG– $\text{KHCO}_3$  compositions in fire suppression was assessed using a sequence of experiments, as outlined in Table 3, encompassing the quantity of sodium employed, duration of extinguishment, and amount of powder consumed. Based on our experiments, we found that the 3:1 EG– $\text{KHCO}_3$  powder was able to put out the sodium fire in just 20 s, using only 6.33 g of powder. The experiments were carried out in controlled conditions to evaluate the fire suppression effectiveness of the powders, with specific emphasis on how the composition of the powders affected the suppression of the sodium fire. The experiments encompassed a range of EG– $\text{KHCO}_3$  concentrations, revealing varying levels of efficacy in suppressing flames caused by sodium metal. The data presented in this study suggest that the EG– $\text{KHCO}_3$  mixes had a notable impact on both the duration of extinguishment and the amount of agent utilized, as compared to the usage of pure EG. It is worth noting that the 3:1 ratio exhibited the most ideal performance. The experimental findings showed that specific ratios, specifically the 3:1 EG– $\text{KHCO}_3$  mixture, enabled a decrease in the amount of substance required to effectively control fires, while maintaining suppression effectiveness. The discovery is noteworthy, indicating that the improved combination proportions enhance the fire-suppression capabilities of the substance, potentially resulting in financial savings and decreased environmental harm. Figure 3 provides a graphic representation of the fire suppression procedure, emphasizing the expeditious suppression obtained with the utilization of EG– $\text{KHCO}_3$  mixtures. When

exposed to a sodium fire, the EG undergoes a rapid transformation into a worm-like structure under elevated temperatures, resulting in a significant increase in volume. This transformation efficiently suppresses the flames by suffocating them. Nevertheless, due to the impact of the flame's plume, the graphite, which resembled a worm-like structure, was propelled into the atmosphere, and scattered. This process was followed by a significant amount of smoke, and remnants of the graphite remained visibly hot, exhibiting red hotspots beneath the layer of EG. This observation implies that the enlarged graphite, due to its low weight, was susceptible to being carried away by the wind, and the layer covering it exhibited significant porosity. If the heat sources were not consistently protected by the agent, the sodium nodules, which are extremely hot, would gradually extend vertically, penetrate the covering layer, and ignite again upon coming into contact with the surrounding air (as depicted in Figure 3a). In comparison to pure EG,  $\text{KHCO}_3$  exhibits notable thermal stability, resistance to decomposition, and the ability to intercalate inside the pores of EG. This intercalation process leads to an increase in the weight of the expanded agent and a reduction in the porosity of EG. In contrast to graphite, the EG- $\text{KHCO}_3$  composite powder demonstrated a significantly faster extinguishing capability for sodium fires, as illustrated in Figure 3b–d. When the quantity of the additional substance was inadequate, it necessitated the use of additional agents and an extended duration during the process of extinguishment (Figure 3b). Nonetheless, it is worth noting that  $\text{KHCO}_3$  exhibits notable porosity and is comparatively less efficient in suppressing fires compared to EG. In cases where an excessive amount of  $\text{KHCO}_3$  is introduced, it might generate several heat sources beneath the covering, potentially causing the flames to reignite (see Figure 3d).

**Table 3.** Experimental data of extinguishing powders.

Powder	Metal Sodium Mass (g)	Extinguishing Time (s)	Agent Mass Consumed (g)	Cooling Rate from 350 to 200 °C (°C/s)	Standard Deviations	
					Extinguishing Time (s)	Agent Mass Consumed (g)
EG	5.45	30	10.00	1.53	2.57	1.79
EG- $\text{KHCO}_3$ (1:1)	5.25	26	12.36	1.44	2.74	2.44
EG- $\text{KHCO}_3$ (3:1)	5.55	20	6.33	2.34	2.00	0.47
EG- $\text{KHCO}_3$ (9:1)	5.55	24	6.55	1.30	2.05	1.25

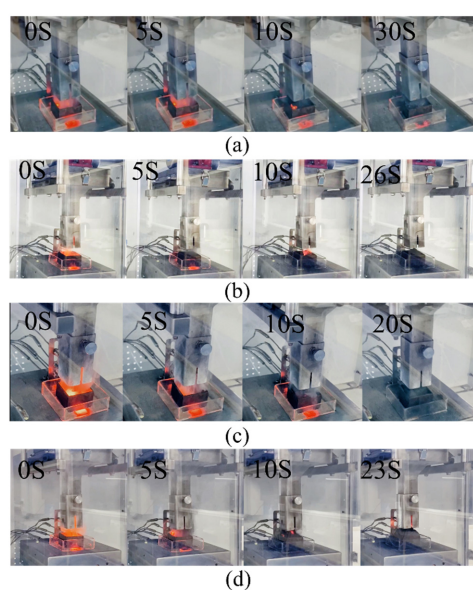


**Figure 3.** Images taken during the fire-extinguishing experiment: (a) EG powder, (b) 1:1, (c) 3:1 and (d) 9:1 EG- $\text{KHCO}_3$  powders.

The process of fire extinguishment was shown to be effective within a time frame of 0–30 s. However, it was noted that there were indications of potential reignition within an extra 10 s observation period. The fire was successfully extinguished using a 1:1 mixture of EG–KHCO<sub>3</sub> within a time frame of 0–26 s. Subsequently, a further 14 s were observed, during which no evidence of reignition was detected. The fire was successfully extinguished using a 3:1 ratio of EG–KHCO<sub>3</sub> within a time frame of 0–20 s. Following the extinguishment, the area was monitored for an additional 20 s, during which no evidence of reignition was noted. The fire was successfully extinguished using a mixture of EG–KHCO<sub>3</sub> in a ratio of 9:1. The extinguishing process took place within a time frame of 0–23 s. Furthermore, the area was monitored for an additional 17 s, during which no indicators of reignition were seen.

### 3.3. Gaseous Product Analysis

The process of heat disintegration in materials, particularly those designed for fire suppression applications, frequently results in the liberation of diverse gases. It is vital to comprehend the inherent characteristics of these gases, including their chemical makeup and the circumstances surrounding their release, in order to evaluate the safety and efficacy of these substances. The present investigation utilized TGA coupled with TG–FTIR to identify and characterize the gaseous breakdown products of the EG–KHCO<sub>3</sub> composite. The findings of this research are illustrated in Figure 4, which displays the spectra acquired at various temperatures throughout the TG–FTIR analysis.

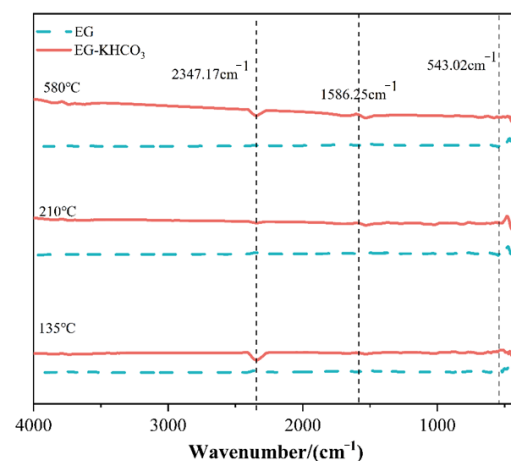


**Figure 4.** Spectra obtained at different temperatures during TG–FTIR analysis.

The TG–FTIR spectra exhibited the existence of multiple discernible peaks that corresponded to various gaseous components. Significantly, the spectral analysis revealed strong peaks at wavenumbers of 2347.17 cm<sup>−1</sup>, 1586.25 cm<sup>−1</sup>, and 543.02 cm<sup>−1</sup>. The spectral peak observed at a wavenumber of 2347.17 cm<sup>−1</sup> is commonly associated with the stretching vibrations of CO<sub>2</sub>. This particular compound is frequently generated as a byproduct during the thermal decomposition of carbonates, such as KHCO<sub>3</sub>. The observed decomposition pathway of KHCO<sub>3</sub> aligns with the anticipated process, wherein the liberation of CO<sub>2</sub> and H<sub>2</sub>O occurs [21].

The absorption peak observed at a wavenumber of 1586.25 cm<sup>−1</sup> can be attributed to the bending vibrations of carbon dioxide or may suggest the existence of carbonates, which are recognized to exhibit absorption in this spectral area. This observation implies the possibility of the existence or formation of a carbonate structure throughout the process of degradation. The peak detected at a wavenumber of 543.02 cm<sup>−1</sup> is of particular significance due to its location within the spectral range associated with vibrations commonly attributed to inorganic substances. The observed phenomenon may be ascribed to the emergence of novel inorganic structures during the process of decomposition, presumably involving potassium remnants resulting from the breakdown of KHCO<sub>3</sub> [5].

The concurrent TG–FTIR research has yielded significant insights into the thermal decomposition characteristics of the composite material consisting of EG and  $\text{KHCO}_3$ . The accurate determination of the gaseous byproducts and their thermal response is of utmost importance in comprehending the material's performance in fire scenarios. The understanding of this information is crucial not only in evaluating the efficacy of the material in suppressing fires but also in guaranteeing its safe utilization, as the gases emitted during decomposition might have significant implications in terms of toxicity and environmental consequences.

### 3.4. Reaction Mechanisms and Energy Pathways

This research study investigated the complex mechanisms involved in the high-temperature decomposition and fire-extinguishing processes of  $\text{KHCO}_3$ . Advanced computational methods, including Gaussian View and Gaussian 16, were employed to visually analyze the reaction pathways, as depicted in Figure 5. Solid lines often represent occupied molecular orbitals or energy levels, whereas dashed lines indicate energy transitions or vacant orbitals and their interactions. The utilization of the B3LYP technique, a computational model for predicting electronic structures, was chosen based on its extensive usage and established credibility in reliably finding stationary point geometries, while also offering computational efficiency and cost-effectiveness. The computational tool employed in this study was B3LYP/TZVP, which is widely recognized for its consistent accuracy in thermodynamic and kinetic evaluations [22].

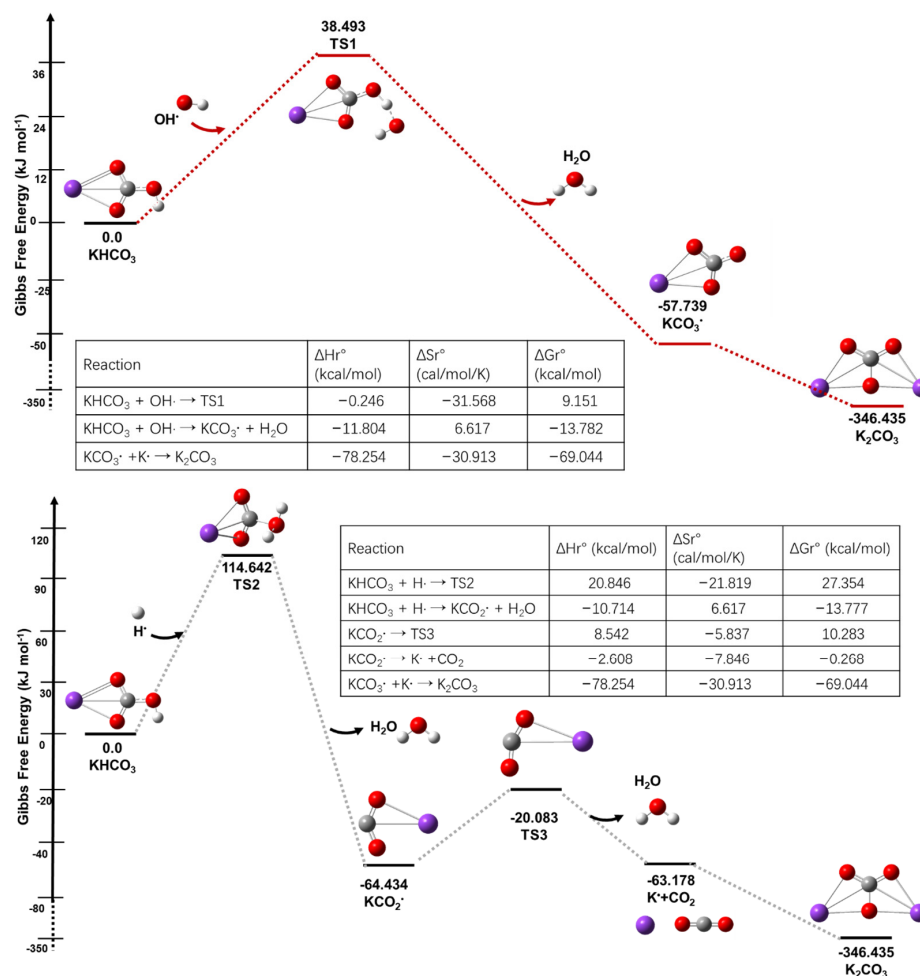
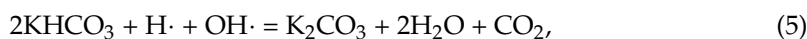
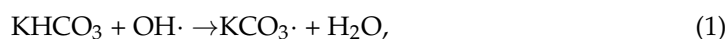


**Figure 5.** Schematic of potential energy of  $\text{KHCO}_3$  reactions (R1, R2). The data along the paths are the relative Gibbs free energy values obtained at the B3LYP/TZVP//CCSD(T)/cc-pVTZ level.

A thorough examination of the frequencies and geometric configurations was carried out for all reactants, transition states, and products, using the B3LYP/TZVP computational method [23]. The DFT-D3BJ approach was additionally employed in order to incorporate dispersion adjustments [24]. The study involved performing vibrational frequency calculations on stationary points, which enabled the determination of both imaginary frequencies for transition states and real frequencies for the equilibrium structures with the lowest energy. In addition, the investigation determined the energy barriers, enthalpy, and entropy of all processes using the B3LYP/TZVP computational method. To obtain more accurate and refined results, the researchers performed single-point energy calculations at the CCSD(T)/cc-pVTZ level. Additionally, zero-point energy corrections were incorporated to account for bond dissociation energies and energy barriers. The utilization of a meticulous computational methodology has yielded noteworthy observations pertaining to the potential energy trajectories and chemical transformations of  $\text{KHCO}_3$ . These findings have made a substantial contribution to our comprehension of its involvement in processes employed to control fires.



### 3.5. Structural Analysis and Visualization

XRD and SEM techniques were employed to investigate the structural characteristics of the EG– $\text{KHCO}_3$  powders. Figure 6 provides a clear depiction of the crystalline properties of the materials by showcasing the XRD patterns. These patterns exhibit well-defined diffraction peaks that serve as evidence for the presence of unique crystalline structures inside the samples. The diffraction pattern of pure EG powder exhibited distinct peaks at  $2\theta$  angles of  $26.4^\circ$  and  $54.7^\circ$  [25]. On the other hand, the EG– $\text{KHCO}_3$  composite exhibited diffraction peaks that closely resembled those of pure EG, indicating that the graphite structure was preserved after the production of the composite. While not all typical peaks of  $\text{KHCO}_3$  were vividly visible, several were recognizable at  $2\theta$  values of  $24.7^\circ$ ,  $29.6^\circ$ ,  $30.4^\circ$ , and  $39.1^\circ$ , confirming the existence of  $\text{KHCO}_3$  within the composite [16,26]. Simultaneously, the SEM pictures provide a comprehensive examination of the surface properties and porosity of the powders, both before and after expansion.

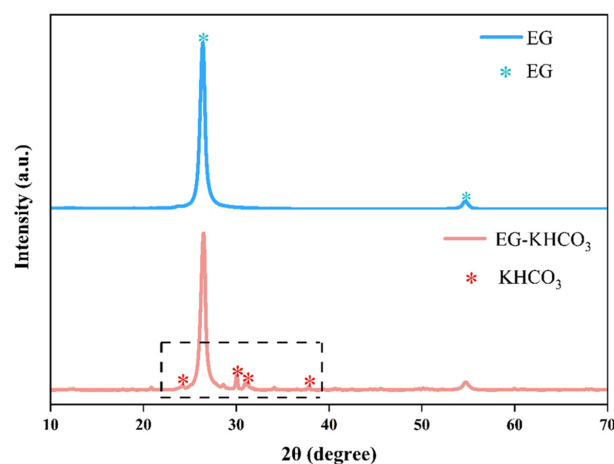


**Figure 6.** XRD pattern of fire extinguishing powder with distinct peaks observed in the dashed line area.

Figure 7 presents a visual comparison of the samples, allowing for a detailed examination [27,28] (Figure 7a). The shown image displays unexpanded EG powder in its pure form, exhibiting a uniformly smooth surface, without any discernible particles or imperfections (Figure 7b). The morphology of pure EG following the expansion process is characterized by the presence of a network-like crisscross of layers and a noticeable porosity. The image labeled as (Figure 7c) illustrates the state of EG–KHCO<sub>3</sub> prior to expansion, exhibiting the presence of minute particulate particles on the surface, which indicates the existence of KHCO<sub>3</sub>. The image in Figure 7d displays EG–KHCO<sub>3</sub> following expansion, with the pores visibly containing particulate debris. This observation provides evidence that KHCO<sub>3</sub> has been well integrated into the EG framework.

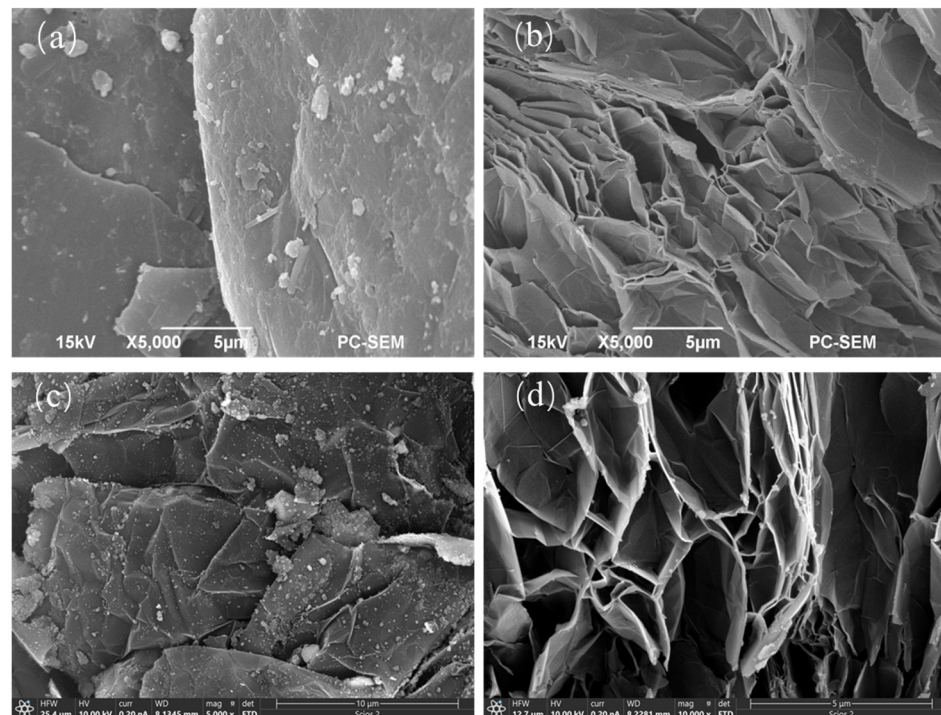


**Figure 7.** SEM images of EG (a,b) and (c,d) EG–KHCO<sub>3</sub> powders.

Through a thorough examination of EG–KHCO<sub>3</sub> compositions, we have discovered a clear and direct relationship between porosity and the effectiveness of fire suppression. Specifically, compositions with a porosity range of 35–40% demonstrated a flame extinguishing rate that was 25% faster compared to compositions with lower porosity values, such as 20–25%. The improved performance is credited to the increased surface area resulting from higher porosity. This allows for better dispersion of the agent and faster absorption of heat during fire suppression operations. The presented photos serve to validate the effective intercalation of KHCO<sub>3</sub> into EG, while also emphasizing the notable structural modifications that arise during expansion. These alterations are of utmost significance in comprehending the fire-suppression properties of the materials.

### 3.6. Temperature Monitoring and Cooling Rate

The thorough execution of temperature monitoring during the fire-suppression trials was accomplished through the utilization of thermocouples [29,30]. The comprehensive outcomes of this monitoring process are visually represented in Figure 8. This figure specifically depicts the temperature change curve acquired by the R1 thermocouple, both during combustion and after fire suppression. The determination of cooling rates within the temperature range of 350 to 200 °C was a pivotal component of the analysis. This metric played a vital role in evaluating the effectiveness of fire-suppression powders in lowering the temperature of metallic sodium after it had been extinguished.

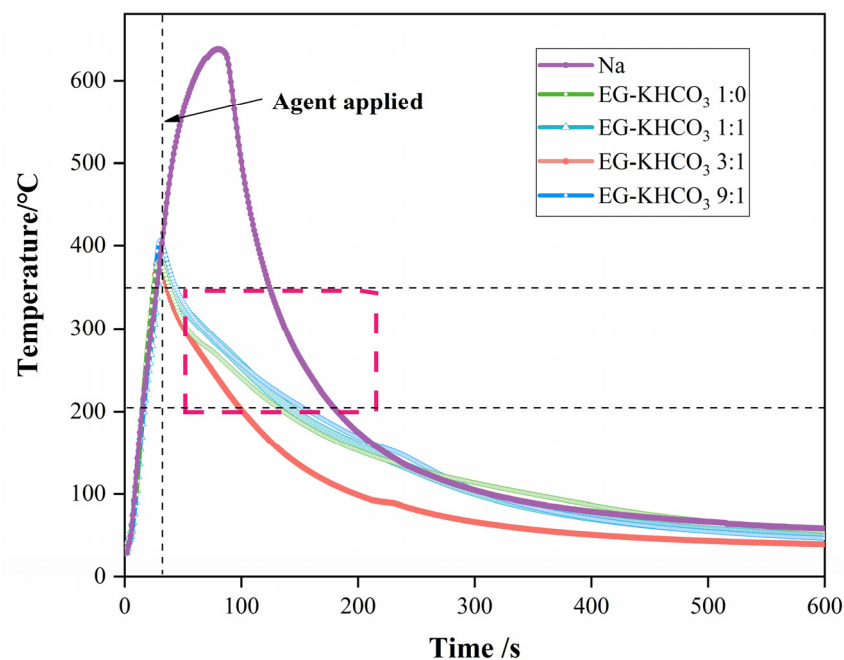


**Figure 8.** Numerical changes measured at thermocouple R1 for the four sample powders during the experiment.

The findings unveiled a clear ranking in the efficiency of cooling across the various compositions. The composite of EG–KHCO<sub>3</sub> at a ratio of 3:1 had the highest cooling rate of 2.34 °C/s, which was significantly superior to the cooling rate of pure EG, at 1.53 °C/s. Subsequently, the compositions of EG–KHCO<sub>3</sub> 1:1 and EG–KHCO<sub>3</sub> 9:1 were examined, revealing cooling speeds of 1.44 °C/s and 1.30 °C/s, respectively. The results of this study highlight the greater effectiveness of the EG–KHCO<sub>3</sub> 3:1 composition in fire suppression. This can be due to its improved ability to cool the affected area after extinguishing the fire. This cooling capacity is crucial in preventing the fire from reigniting and ensuring that the fire is fully mitigated.

#### 4. Conclusions

The present study investigated the dynamics of fire suppression by utilizing compositions of EG and KHCO<sub>3</sub>. The findings of this research have significant implications for fire safety and emergency response, particularly in the context of metal fires. The data presented in this study are the result of a comprehensive and meticulous process of trials and analyses. The present study provides a thorough examination of the potential of EG–KHCO<sub>3</sub> compositions as highly efficient fire-extinguishing agents. Emphasis is placed on their thermal stability, decomposition characteristics, and exceptional performance in fire suppression studies. This work establishes a foundation for future investigations into innovative fire-suppression materials and tactics.

The investigation unequivocally proved that compositions containing EG–KHCO<sub>3</sub>, particularly in a 3:1 ratio, display improved thermal properties and effectiveness in suppressing fires, especially those involving metals. The 3:1 EG–KHCO<sub>3</sub> mixture effectively decreased the time required to extinguish fires to 20 s and demonstrated efficient utilization of resources, with a mere 50 g of the agent being used. FTIR spectroscopy and XRD, SEM analyses have verified that KHCO<sub>3</sub> has been successfully incorporated into the EG matrix, resulting in improved resistance to heat and increased chemical reactivity. Significantly, the mixture with a ratio of 3:1 also demonstrated exceptional effectiveness in rapidly reducing the temperature after a fire, achieving a cooling rate of 2.34 °C/s, from 350 to 200 °C. The results highlight the potential of EG–KHCO<sub>3</sub> in fire prevention applications, but additional research is required to evaluate its wider applicability and environmental impact.

**Author Contributions:** Conceptualization, A.-C.H.; methodology, X.-Y.M.; software, F.-C.C.; formal analysis, F.-C.C. and X.-Y.M.; investigation, F.-C.C. and X.-Y.M.; resources, A.-C.H.; data curation, F.-C.C.; writing—original draft preparation, A.-C.H.; writing—review and editing, A.-C.H. All authors have read and agreed to the published version of the manuscript.

**Funding:** This research received no external funding.

**Data Availability Statement:** The data presented in this study are available on request from the corresponding authors.

**Conflicts of Interest:** The authors declare no conflicts of interest.

## References

1. Bai, X.; Sun, P.; Luo, G.; Cao, H.; Wei, X. Large Leakage Sodium-Water Reaction Accident Analysis in a Sodium-Cooled Fast Reactor with Paralleling Steam Generators. *Prog. Nucl. Energy* **2023**, *162*, 104770. [[CrossRef](#)]
2. Yan, L.; Wang, N.; Xu, Z. Experimental Study on the Effectiveness and Safety of Cement Powder on Extinguishing Metal Magnesium Fires Based on Pneumatic Conveying Technology. *Case Stud. Therm. Eng.* **2022**, *37*, 102279. [[CrossRef](#)]
3. Jiang, H.; Jiang, Y.; Fan, R. Extinguishing Capability of Novel Ultra-Fine Dry Chemical Agents Loaded with Iron Hydroxide Oxide. *Fire Saf. J.* **2022**, *130*, 103578. [[CrossRef](#)]
4. Zhang, Y.; Wang, Z.; Liu, J.; Li, Q.; Pan, R.; Zhou, X. Alkaline Potassium Aluminum Carbonate: A Novel High-Efficiency Dry Powder Extinguishing Agent with High Heat-Resistant. *J. Anal. Appl. Pyrolysis* **2023**, *173*, 106038. [[CrossRef](#)]
5. Zhao, J.; Fu, Y.; Lu, S.; Lu, G.; Xue, F.; Zhang, H. An Improved Method to Determine the Minimum Extinguishing Concentrations of Ultrafine Dry Powder Agents: Taking  $\text{NaHCO}_3$  and  $\text{KHCO}_3$  as Examples. *Process Saf. Environ. Prot.* **2023**, *172*, 846–856. [[CrossRef](#)]
6. Lonergan, J.; Goncharov, V.; Swinhart, M.; Makovsky, K.; Rollog, M.; McNamara, B.; Clark, R.; Cutforth, D.; Armstrong, C.; Guo, X.; et al. Thermodynamic Investigation of the NaCl-KCl Salt System from 25 to 950 °C. *J. Mol. Liq.* **2023**, *391*, 122591. [[CrossRef](#)]
7. Huang, L.; Jiang, H.; Zhang, T.; Shang, S.; Gao, W. Effect of Superfine  $\text{KHCO}_3$  and ABC Powder on Ignition Sensitivity of PMMA Dust Layer. *J. Loss Prev. Process Ind.* **2021**, *72*, 104567. [[CrossRef](#)]
8. Baldissera, A.F.; Silveira, M.R.; Beraldo, C.H.; Tocchetto, N.S.; Ferreira, C.A. Evaluation of the Expandable Graphite/Polyaniline Combination in Intumescent Coatings. *Synth. Met.* **2019**, *256*, 116141. [[CrossRef](#)]
9. Tsai, Y.T.; Yang, Y.; Pan, Y.; Shu, C.M. Catalytic Effects of Magnesium-Transition Metal (Fe and Ni) Hydrides on Oxygen and Nitrogen Reduction: A Case Study of Explosive Characteristics and Their Environmental Contaminants. *Energy* **2023**, *280*, 128222. [[CrossRef](#)]
10. Wang, S.; Tan, L.; Xu, T. Synergistic effects of developed composite flame retardant on VOCs constituents of heated asphalt and carbonized layer compositions. *J. Clean. Prod.* **2022**, *367*, 133107. [[CrossRef](#)]
11. Huang, C.F.; Chen, W.T.; Kao, C.K.; Chang, H.J.; Kao, P.M.; Wan, T.J. Application of Fuzzy Multi-Objective Programming to Regional Sewer System Planning. *Processes* **2023**, *11*, 183. [[CrossRef](#)]
12. Ni, X.; Zheng, Z. Extinguishment of Sodium Fires with Graphite@Stearate Core-Shell Structured Particles. *Fire Saf. J.* **2020**, *111*, 102933. [[CrossRef](#)]
13. Wang, S.; Xu, Z.; Xu, T. Improving the controlled-release effects of composite flame retardant by loading on porous attapulgite and coating. *Ceram. Int.* **2023**, *49*, 7871–7887. [[CrossRef](#)]
14. Liu, A.; Lu, X.; Zhou, X.; Xu, C.; Liang, X.; Xiong, K. Experimental Investigation on Suppression of Methane Explosion Using  $\text{KHCO}_3$ /Zeolite Composite Powder. *Powder Technol.* **2023**, *415*, 118157. [[CrossRef](#)]
15. Liu, J.W.; Xiao, Y.; Wang, Z.P.; Li, Q.W. Electron heat transport in low-rank lignite: Combining experimental and computational methods. *J. Therm. Anal. Calorim.* **2023**, *148*, 4759–4768. [[CrossRef](#)]
16. Ma, X.Y.; Cao, F.C.; Zhou, H.L.; Liu, Y.C.; Tang, Y.; Kang, Q.C.; Shu, Z.J.; Dong, X.L.; Huang, A.C. Experimental Investigation of the Performance of Modified Expanded Graphite Powder Doped with Zinc Borate in Extinguishing Sodium Fires. *J. Loss Prev. Process Ind.* **2023**, *84*, 105110. [[CrossRef](#)]
17. Zhang, M.L.; Dong, X.L.; Tang, Y.; Huang, A.C.; Chen, F.; Kang, Q.C.; Shu, Z.J.; Xing, Z.X. Experimental Investigations of Extinguishing Sodium Pool Fires Using Modified Expandable Graphite Powders. *Case Stud. Therm. Eng.* **2022**, *32*, 101911. [[CrossRef](#)]
18. Cao, F.C.; Ma, X.Y.; Zhou, H.L.; Tang, Y.; Dong, X.L.; Huang, A.C. Enhanced Suppression of Metal Combustion Processes Using a Compound Expansible Graphite Extinguishing Agent: Experimental Study and Mechanistic Insights. *J. Loss Prev. Process Ind.* **2023**, *85*, 105154. [[CrossRef](#)]
19. Hu, W.; Yu, R.; Chang, Z.; Tan, Z.; Liu, X. The Fire Extinguishing Mechanism of Ultrafine Composite Dry Powder Agent Containing  $\text{Mg}(\text{OH})_2$ . *Int. J. Quantum Chem.* **2021**, *121*, e26810. [[CrossRef](#)]
20. Wang, Y.Q.; Xie, L.J.; Sun, H.Q.; Wang, X.; Zhou, H.L.; Tang, Y.; Jiang, J.C.; Huang, A.C. 4,5-Difluoro-1,3-dioxolan-2-one as a film-forming additive improves the cycling and thermal stability of SiO/C anode Li-ion batteries. *Process Saf. Environ. Prot.* **2024**, *183*, 496–504. [[CrossRef](#)]

21. Jinzhang, J.; Xiuyuan, T.; Fengxiao, W. Study on the Effect of  $\text{KHCO}_3$  Particle Size and Powder Spraying Pressure on the Methane Explosion Suppression Characteristics of Pipe Networks. *ACS Omega* **2022**, *7*, 31974–31982. [[CrossRef](#)] [[PubMed](#)]
22. Zhang, C.; Li, H.; Guo, X.; Li, S.; Zhang, H.; Pan, X.; Hua, M. Experimental and Theoretical Studies on the Effect of  $\text{Al}(\text{OH})_3$  on the Fire-Extinguishing Performance of Superfine ABC Dry Powder. *Powder Technol.* **2021**, *393*, 280–290. [[CrossRef](#)]
23. Řezáč, J. Non-Covalent Interactions Atlas Benchmark Data Sets 2: Hydrogen Bonding in an Extended Chemical Space. *J. Chem. Theory Comput.* **2020**, *16*, 6305–6316. [[CrossRef](#)]
24. Tang, Y.; Sun, H.; Liu, J.; Zhang, D.; Wang, R.; Dai, J. Computational Study on the Mechanisms and Reaction Pathways of the  $\text{CX}_3\text{O}_2 + \text{Br}$  ( $X=\text{F}$  and  $\text{Cl}$ ) Reactions. *J. Fluor. Chem.* **2013**, *153*, 130–136. [[CrossRef](#)]
25. Lin, S.; Dong, L.; Zhang, J.; Lu, H. Room-Temperature Intercalation and ~1000-Fold Chemical Expansion for Scalable Preparation of High-Quality Graphene. *Chem. Mater.* **2016**, *28*, 2138–2146. [[CrossRef](#)]
26. Zhou, J.; Li, B.; Ma, D.; Jiang, H.; Gan, B.; Bi, M.; Gao, W. Suppression of Nano-Polymethyl Methacrylate Dust Explosions by ABC Powder. *Process Saf. Environ. Prot.* **2019**, *122*, 144–152. [[CrossRef](#)]
27. Meng, F.; Amyotte, P.; Hou, X.; Li, C.; He, C.; Li, G.; Yuan, C.; Liang, Y. Suppression Effect of Expandable Graphite on Fire Hazard of Dust Layers. *Process Saf. Environ. Prot.* **2022**, *168*, 1120–1130. [[CrossRef](#)]
28. Roosendans, D.; Van Wingerden, K.; Holme, M.N.; Hoorelbeke, P. Experimental Investigation of Explosion Mitigating Properties of Aqueous Potassium Carbonate Solutions. *J. Loss Prev. Process Ind.* **2017**, *46*, 209–226. [[CrossRef](#)]
29. Qu, J.; Deng, J.; Luo, Z.M.; Xiao, Y.; Shu, C.M. Thermal Reaction Characteristics and Microstructure Evolution of Aluminium Nano-Powder in Various Mixtures of Oxygen and Nitrogen Atmosphere. *Process Saf. Environ. Prot.* **2023**, *170*, 45–53. [[CrossRef](#)]
30. Zhang, Y.; Xu, K.; Li, J.; Liu, B.; Wang, B. Hydrogen inhibition effect of chitosan and sodium phosphate on ZK60 waste dust in a wet dust removal system: A feasible way to control hydrogen explosion. *J. Magnes. Alloys* **2023**, *11*, 2916–2926. [[CrossRef](#)]

**Disclaimer/Publisher's Note:** The statements, opinions and data contained in all publications are solely those of the individual author(s) and contributor(s) and not of MDPI and/or the editor(s). MDPI and/or the editor(s) disclaim responsibility for any injury to people or property resulting from any ideas, methods, instructions or products referred to in the content.